


A nano based approach to alleviate cisplatin induced nephrotoxicity

Lobna M Anees¹ , Gehan R Abdel-Hamid² and Ahmed A Elkady¹

International Journal of
Immunopathology and Pharmacology
Volume 35: 1–14
© The Author(s) 2021
Article reuse guidelines:
sagepub.com/journals-permissions
DOI: 10.1177/20587384211066441
journals.sagepub.com/home/iji


Abstract

Background and objective: Cisplatin, an effective drug against cancer, commonly induces nephrotoxicity; limiting its therapeutic efficacy and application. In this study, Cisplatin NanoComposite (Cis NC) was formulated successfully from irradiated chitosan coated Cisplatin and MgO nanoparticles (CHIT/Cis/MgO NPs) to promote cisplatin release in a more sustained manner to improve therapeutic efficacy via the reduction of its nephrotoxicity. To compare the relative induced renal toxicity of cisplatin with Cisplatin NanoComposite, histological and biochemical mechanisms underlying nephrotoxicity were investigated.

Methods: Thirty rats were equally separated to three groups, first group received saline injections and adjusted as the control group, the second group was injected intra-peritoneal with cisplatin 0.64 mg/kg b. wt./day for 6 weeks, the third group was injected intra-peritoneal with Cis NC 5.75 mg/kg b. wt. daily for 6 weeks.

Results: Cisplatin-induced renal functional impairment and histopathological damages in the kidney; also, cisplatin disrupted the balance of the redox system in renal tissue, stimulated the inflammatory reactions in the kidney via triggering signal transducer and activator of transcription-I (STAT1) dependent pathways. Moreover, Cisplatin-induced activation of mammalian target of rapamycin mTOR and inactivation of AMPK/PI3K/Akt signal pathway, and was coupled with induction of p53 activity and the executioner caspase3 to induce apoptotic renal cell death. On the other hand, Cis NC exerted a minimal stimulatory effect on apoptotic and inflammatory signal cascade with negligible renal functional and morphological alterations.

Conclusion: We postulated that Cis NC may be a valued possible drug to decrease the cytotoxicity of cisplatin thus reserves the renal function and structure.

Keywords

Cisplatin nanocomposite, cisplatin, nephrotoxicity

Date received: 18 September 2021; accepted: 24 November 2021

Introduction

Cisplatin is commonly applied in the treatment of a diversity of solid tumors in medical practice due to its simple administration and great efficacy.¹ Cisplatin efficiency is proportionate to its dose. Nevertheless, cisplatin has a relatively limited safety margin and exhibits significant dose-limiting side effects, such as vomiting, nausea, ototoxicity, neurotoxicity, and particularly nephrotoxicity.² Hence, there is an urgent

¹Health Radiation Research Department, National Center for Radiation Research and Technology (NCRRT), Egyptian Atomic Energy Authority (AEA), Cairo, Egypt

²Radiation Biology Department, National Center for Radiation Research and Technology (NCRRT), Egyptian Atomic Energy Authority (AEA), Cairo, Egypt

Corresponding author:

Lobna M Anees, Health Radiation Research Department, National Center for Radiation Research and Technology (NCRRT), Egyptian Atomic Energy Authority (AEA), Ahmed el Zomor Street, Cairo 11865, Egypt.
Email: Lobnaanis@gmail.com



Creative Commons Non Commercial CC BY-NC: This article is distributed under the terms of the Creative Commons Attribution-NonCommercial 4.0 License (<https://creativecommons.org/licenses/by-nc/4.0/>) which permits non-commercial use, reproduction and distribution of the work without further permission provided the original work is attributed as specified on the SAGE and Open Access pages (<https://us.sagepub.com/en-us/nam/open-access-at-sage>).

need to minimize renal damage in patients treated with cisplatin, also the cisplatin pathogenesis must be explained to create a novel medicine to mitigate cisplatin induced nephrotoxicity.³

Platinum composite loaded polymeric carrier has been formulated for passive and active targeting.⁴ To improve and manipulate limitations of traditional chemotherapies, nanoparticles have been designed and formulated with optimum size and surface characteristics to be loaded with active anticancer drugs, chitosan is a flexible transporter for gene and drug delivery. This is accredited to the reactive amino group of glucosamine in the C2 position, which could easily be used for chemical alteration, binding with medications and cell or tissue targeting moieties, and forming complexes with DNA, short interfering RNA, and oligonucleotides.⁵

In recent years, the pathophysiological basis and the molecular mechanism underlying cisplatin mediated kidney damage have been elucidated. A previous study⁶ illustrated that cytotoxicity endpoint is indicated by toxicity markers which include the formation of reactive oxygen species, depletion of antioxidant enzymes, lysosomal and mitochondrial membrane damage, stimulation of apoptosis-related gene expression, and finally cell death. There is a confirmed indication that inflammation, oxidative stress, apoptosis, and necrosis can play critical roles in cisplatin provoked renal toxicity.⁷

Current evidence proposes that cisplatin penetrates cells causing mitochondrial dysfunction and lipid peroxidation yields accumulation in renal tissues, leading to fast production of reactive oxygen species (ROS) moreover activating the oxidative metabolic system. Accumulation of ROS above inadequate antioxidant mechanism consequences in the diminution of glutathione (GSH), superoxide dismutase (SOD), and a rise in MDA level in addition to the enhancements of inflammatory factors including iNOS, NF- κ B, Tumor Necrosis Factor- α , and interleukin-1 β .⁸ The pro-inflammatory cytokines production, mitochondrial dysfunction also defects in the PI3K/Akt cellular pathway, collectively trigger the apoptosis signaling pathway.⁹ Previous studies indicated that cisplatin induced excessive renal cell death and kidney damage which can be efficiently improved via regulating AMP-activated protein kinase (AMPK) also its downstream PI3K/Akt as well as p53 signal pathways.^{10,11} AMPK is a main metabolic switch, which is essential for cells to preserve the regular energy metabolic rate and redox equilibrium.¹² Therefore, AMPK activation may ameliorate cisplatin induced kidney damage.^{13,14} PI3K, the main downstream target of AMPK, regulates cellular characteristics such as proliferation, survival, and apoptosis^{15,16} via phosphorylation of Akt.^{17,18}

The cytoplasmic transcription factor STAT1 participates in the signal cascade triggered via cellular stress and

cytokines. Those signals facilitate its phosphorylation and translocation toward the nuclei, where it controls genes associated with inflammation, for instance; inducible nitric oxide synthase,¹⁹ TNF- α ,²⁰ also genes involved in apoptosis, for example, Fas, caspases, and TNF-related apoptosis-inducing ligand (TRAIL).²¹ STAT1 also induces apoptosis in association with the cell cycle regulator p53.²² Interestingly, STAT1 knockdown by Short interfering RNA (siRNA) against STAT1 alleviated cisplatin-mediated activation of p53, indicating that p53 activity is regulated by STAT1.²³

In this study, the treatment with Cisplatin NanoComposite (Cis NC) relatively reduced the toxic effect of free cisplatin on renal tissue. It was revealed that treatment with Cis NC limited the inflammation, apoptosis, and oxidative stress by regulating AMPK/PI3K/Akt - mTOR as well as STAT1/p53 signal pathways thus reserved renal tissue from damage.

Materials and methods

Chemicals

Chitosan (CHIT) with an average Mwt (100,000–300,000) was supplied by Sigma Co. USA. Magnesium nitrate hexahydrate (MgNO₃.6H₂O), NaOH, and other reagents were graded analytically and they were used as it is without any treatment, provided by Acmatic Co. Egypt. Urethane was obtained from Sigma Aldrich Corporation (USA). Cisplatin (cisPtCl₂ (NH₃)₂) was acquired from Oncotec Pharma company.

Steps of preparation of Cisplatin NanoComposite (Cis NC)

Preparation of Magnesium Oxide NPs coated with CHIT

First, to prepare a 1% CHIT solution, 1gm of chitosan was dissolved in a 1% acetic acid solution (100 mL) and vigorously stirred with a magnetic stirrer till completely homogenate. Next, thoroughly combine equal volumes of CHIT and magnesium nitrate solution (1M) by stirring for 1h and 30 min. Then 20 mL of Cisplatin (Cis) was added and the stirring continued for 1 hour. To the chitosan/magnesium nitrate/cisplatin mixture solution, add 40 mL of Na OH solution (1M) drop-wise and very gradually till the formation of a milky white suspension.

Radiation facility

The MgO/CHIT/Cis milky white dispersion then exposed to 10 kGy dose of γ -radiation using the ¹³⁷Cesium source (gamma cell-40) available at The National Center for Radiation Research and Technology (NCRRT), Egyptian Atomic Energy Authority (Cairo, Egypt), manufactured by Canadian Atomic Energy Co., Ltd (Ontario, Canada). Gamma radiation exposure will break down the CHIT

molecular chains to a very low molecular weight, ensuring CHIT coating of Cisplatin and Magnesium Oxide NC. The formed precipitate after irradiation is washed several times by decantation for 2 days to ensure the removal of excess Na OH, the suspended mixture of MgO/CHIT/Cis was placed in a clean container and cautiously sealed till used.

Characterizations of MgO/CHIT and MgO/CHIT/Cis nanocomposite. The IR study of MgO/CHIT and MgO/CHIT/Cis nanocomposite samples were verified by Fourier-Transform Infrared Spectroscopy-Vertex 70 spectrophotometer (Bruker, Germany). Transmission Electron Microscopy (TEM) was applied to evaluate the bulk and shape of the prepared MgO/CHIT NPs. The formed nanoparticles powder was suspended in doubly distilled water then dispersions were dropped on an ultrathin carbon-reinforced copper grid and dehydrated in an oven overnight. TEM JEOL: JEM-100cx was applied for this determination. The X-ray diffractogram for Magnesium Oxide NPs was obtained by Rigaku 2550D/max VB/PC X-ray diffractometer.

Animals

Male Wister rats (of approximate weight 110–120 g) were acquired from the Nile Pharmaceutical Company, Cairo, Egypt. The rats were kept in the animal facility of the National Center for Radiation Research and Technology, Cairo, Egypt. Before beginning the experiment the rats were kept to adapt for a week. They were kept under standard laboratory conditions of light/dark cycle (12/12 h) at a temperature of $25 \pm 2^\circ\text{C}$ and humidity of $60 \pm 5\%$. The rats were accommodated in cages with free access to drinking water and food. Rats were provided with suitable standard laboratory food (pellets). All animal experiments were carried out in accordance with the National Institutes of Health guide for the Care and Use of Laboratory Animals (serial:18–2019) in accordance with international ethical considerations.

Experimental design

Thirty rats were randomly separated to three main equal groups, 10 rats each, kept in separate cages and categorized as follow:

a. Group 1: Normal control group

Rats received normal saline, designated as an untreated control group.

b. Group 2: Cisplatin intoxicated group

Rats were treated 0.64 mg/kg b. wt. daily for 6 weeks, the choice of the dose was according to $1/10 \text{ LD}_{50}$ injected intra-peritoneal

c. Group 3: Cis NC treated group

Rats were treated 5.75 mg/kg b. wt. daily for 6 weeks the choice of the dose was according to $1/10 \text{ LD}_{50}$ injected intra-peritoneal

By the end of the experiment, rats were anesthetized by ether to withdraw blood samples from the heart of each rat. Blood samples were permitted to clot and formerly were centrifuged for 15 min at 3000 r/min. Then, rats were sacrificed via cervical dislocation; part of the kidneys were quickly dissected, washed with ice-cold saline, dried, and weighed for biochemical analysis. Another part of the kidney was separated and was reserved for histopathological investigation.

Determination of kidney function

Serum urea and creatinine were measured by bio-diagnostic kits (Cairo, Egypt)

Determination of oxidative stress markers

Lipid peroxidation end products in kidney tissue homogenate were estimated via the thiobarbituric acid (TBA) test for malondialdehyde (MDA), following the method described by Yoshioka et al.²⁴ Reduced glutathione (GSH) contents were measured as defined by Beutler et al.²⁵

Determination of 8-OHdG, iNOS, and NADPH oxidase

ELISA kits (BioSource Int., Camarillo, California, United States) were used to determine levels of 8-OHdG, iNOS, and NADPH oxidase on kidney tissue homogenate consistent with the manufacturer's protocol.

Determination of caspase3, interleukin-1 β , and Tumor Necrosis Factor-alpha

The collected serum was used to determine concentrations of IL-1 β , and TNF-alpha in addition to tissue caspase3 using ELISA technique (BioSource Int., Camarillo, California, United States) as described by the protocol supplied via the manufacturer.

Estimation of Nuclear factor kappa B, STAT1, and P53 gene expression in kidney tissue homogenate via quantitative real-time polymerase chain reaction (qPCR)

Extraction of RNA and synthesis of cDNA. To examine the alterations in mRNA expression for NFkB, STAT1, and P53, TRIzol reagent (Life Technologies, USA) was used to

Table 1. Primers list used in polymerase chain reaction.

Gene	Primer sequence	Gene bank accession numbers
NFkB	F: 5'-GCTTACGGTGGGATTGCATT-3' R: 5'-TTATGGTGCCATGGGTGATG-3'	>XM_006233360.3
STAT1	F: 5'- GGGCGTCTATCCTGTGGTAC-3' R: 5'- CTGCCAACTCAACACCTCTG-3'	>NM_032612.3
P53	F: 5'- GTCGGCTCCGACTATACCACTATC-3' R: 5'- CTCTCTTTGCACTCCCTGGGGG -3'	>NM_030989.3
β -actin	F: 5'- TCTGGCACCACACCTTCTACAATG-3' R: 5'- AGCACAGCCTGGATAGCAACG -3'	>NM_031144.3

isolate total RNA from 50 mg kidney tissue. Reverse transcriptase (Invitrogen) was used to synthesize complementary DNA (cDNA) first strand using 1 mg RNA template.

Reverse transcription-polymerase chain reaction (RT-PCR). The Sequence Detection Software (PE Biosystems, CA) was used to perform RT-PCRs in a step-one plus thermal cycler (Applied Biosystems, Waltham, MA, USA). [Table 1](#)) shows the list of oligonucleotides utilized in this research. 25 μ L entire volume of the reaction mix consists of 2 μ L of cDNA, 900 nM of each primer, and two SYBR Green PCR Master Mix (Qiagen, catalog number/ID: 204 143). The PCR thermal cycling conditions involved an initial denaturation phase for 5 min at 95°C; then 40 cycles for 20 s at 95°C, followed by 60°C for 1min for annealing and extension. The comparative Ct method was used to calculate the mRNA gene expression of NFkB, STAT1, and P53 as described by Pfaffl.²⁶ Calculations were carried out by normalizing the mean Ct value of each treatment relative to the β -actin endogenous control by calculating the $2^{-\Delta\Delta Ct}$ values.

Western immunoblotting

TRIzol reagent (Invitrogen) was used to extract proteins from kidney tissue in accordance with the protocol supplied via the manufacturer (ThermoFisher). Each lane was loaded with 20 μ g of protein and separated by 10% sodium dodecyl sulfate–polyacrylamide gel electrophoresis (SDS-PAGE) then transferred onto polyvinylidene difluoride (PVDF) membrane. Membranes were blocked with blocking solution containing 5% non-fat milk for 2h at room temperature then were washed with Tris-buffered saline with Tween 20 (TBS-T), and then incubated overnight at 4°C with primary antibodies toward AMPK, p-AMPK, PI3K, p-PI3K, Akt, p-Akt, mTOR, p-mTOR, and β -actin was used as a loading control. The membranes were washed several times with TBS-T before being incubated with horseradish peroxidase-conjugated

secondary monoclonal antibodies for 2h at room temperature then were washed several times with TBS-T. Using Amersham detection kit to develop and visualize membranes by chemiluminescence in accordance with the manufacturer's instructions before being exposed to X-ray film. Primary and secondary antibodies were acquired from Cell Signaling Technology (USA). Densitometric analysis of the autoradiograms was used to quantify AMPK, p-AMPK, PI3K, p-PI3K, Akt, p-Akt, and mTOR, p-mTOR proteins, using a scanning laser densitometer (Biomed Instrument Inc., USA). All values were normalized to β -actin and results were expressed as arbitrary units.

Histopathological examination

A histological examination was performed on renal tissue specimens from each study group to identify and compare the histological alterations that resulted from Cisplatin and Cis NC treatment. Tissue samples were fixed with 10% buffered formalin, dehydrated with a gradient concentration of alcohol, and immersed in xylene, then embedded in paraffin. A microtome (Leica, Germany) was used to take 5- μ m thick sections of each tissue sample on glass slides. After clearing paraffin, the sections were stained with hematoxylin then counterstained with Eosin to be analyzed microscopically below the light microscope at original magnification of $\times 400$, and the images were obtained by a digital camera (Nikon, ECLIPSE, TS100, Japan).

Statistical analysis

The data analysis was performed using SPSS (version 20) to analyze the data by one-way analysis of variance (-ANOVA). After that a post hoc test (LSD) for multiple comparisons was performed. The obtained data were expressed as mean \pm standard error (SE). Considering p values <0.05 were statistically significant. G-power statistical program²⁷ was used to calculate sample size.

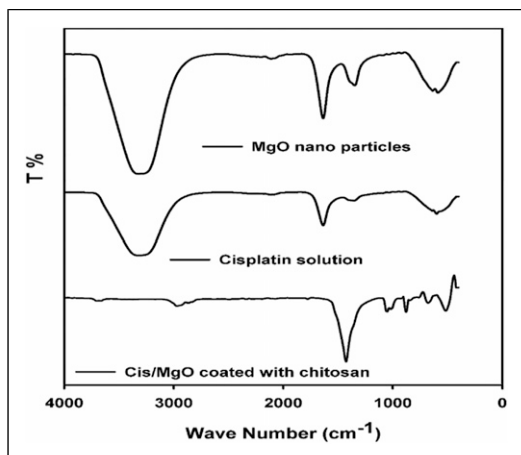


Figure 1. IR spectroscopy of MgO NPs, Cisplatin, and Magnesium Oxide/Cisplatin coated with chitosan.

Results

Chemical evaluations

Characterization of MgO/CHIT and MgO/CHIT/cisplatin nanocomposite

IR spectrum of cisplatin and MgO/CIS coated with chitosan. The characteristic IR bands for the MgO NPs, Cisplatin (Cis), and MgO/Cis coated with chitosan are illustrated in Figure 1. From infrared analysis of the Cis sample, the chief bands appeared due to extending vibrations of the OH group at 3326.5 cm^{-1} because of moisture content, and the stretching vibration at a range of 582.8 cm^{-1} to 603.9 due to the Pt-O-Pt linkage. The IR of MgO nano dispersion demonstrates a stretching vibration manner that appears in the range of $587\text{--}633\text{ cm}^{-1}$ was attributed to the Mg-O-Mg interactions. Two separate bands are noticed around $968.8\text{--}1636\text{ cm}^{-1}$, which are associated to the bending vibration of hydroxyl group provided by absorbed water molecules on the surface of the prepared particle samples. The stretching vibration of the OH group appeared at 3289.4 cm^{-1} .²⁸ The appearance of the OH bands was owing to the adsorbed moisture on the MgO surface.

IR spectrum of magnesium oxide/Cisplatin coated with chitosan (MgO/Cis/CHIT) as shown in Figure 1 represents a combination of all constituents of the prepared nanocomposite sample, where the characteristic bands of CHIT were observed at: 3360 cm^{-1} (for the OH groups), 2972 cm^{-1} (for C-H group), 1777 cm^{-1} (for the amide carbonyl groups), 1424 cm^{-1} (for CH₂ bending vibration), and 1059 cm^{-1} (for C=O group), (Figure 1). The appearance of these bands confirms the preservation of the CHIT characteristic structural features after the embedding of the MgO/Cis NPs within the polymeric matrix. Furthermore, a noticeable shift in the IR bands of CHIT-MgO NC resulted

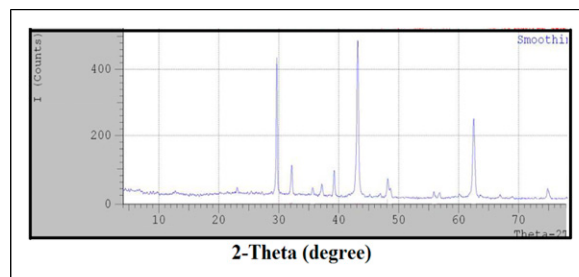


Figure 2. XRD pattern of pure MgO NPs.

from the influence of embedded magnesium oxide NPs due to their interaction with CHIT chains. These observed shifts are especially because of the interaction between the NH and OH groups, confirming the H-bonding interaction of these groups with magnesium oxide molecules.

X-ray diffraction. The X-ray diffractogram of prepared MgO nanoparticles is illustrated in (Figure 2) which confirms that the synthesized MgO is of hexagonal structure²⁹ detected with no impurities. The average size of the prepared nanoparticles was estimated to be 4.3 nm using Scherer formula: Crystallite average size $D = k \lambda / \beta (\cos \theta)$

Where D is the crystallite size in nm, λ is the radiation wavelength (0.154 nm for Cu K), β is the bandwidth at half-height and θ is the diffraction peak angle and k is a constant (0.9). After a correction for the instrumental broadening, the average value of the magnesium oxide NPs size was found to be 4.26 nm.

Transmission electron microscopy of MgO NPs. Transmission electron microscopy (TEM) is the best applicable technique used to evaluate and investigate the morphology of materials, and to conclude the magnitude of molecular spots at the nanoscale. MgO samples were shown by TEM images in (Figure 3). The TEM images of MgO nanoparticles (Figure 3) show a systematic structure of MgO nanoparticles and also demonstrate that the MgO nanocrystallites have equivalent lamellar morphologies with a hexagonal shape and the sizes of the particles vary, giving an average size of nearly 10.32 nm.

Biochemical studies

The effect of Cis NC or cisplatin on kidney function. To investigate the renal dysfunction induced by Cis NC or cisplatin, we measured the serum levels of creatinine and urea in male rats treated by cisplatin or Cis NC. As shown in Table 2, the treatment of rats by cisplatin induced a pronounced elevation in serum urea and creatinine. However, no significant changes were observed in the case of rats treated with Cis NC as compared to control.

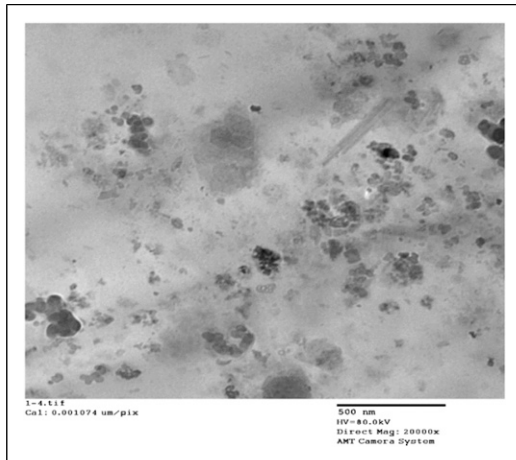


Figure 3. TEM photo of MgO NPs (dispersion).

The effect of Cis NC or cisplatin on oxidative stress biomarkers in renal tissue. Administration of cisplatin or Cis NC led to a significant rise in the prooxidant indicator; MDA, and oxidative DNA damage indicator 8-hydroxy-2'-deoxyguanosine (8-OHdG), in addition to significant decreases in antioxidant molecules (GSH) in the kidneys of male rats as compared with equivalent values in normal tissues (Table 3). The data obtained revealed the changes in the measured parameters are more pronounced in the case of the cisplatin group when compared to the Cis NC treated rats.

The effect of Cis NC or cisplatin on the levels of NADPH oxidase and iNOS in renal tissue. To identify whether oxidative stress is associated with the progress of cisplatin induced kidney injury, we measured the levels of NADPH oxidase and iNOS in all groups. An apparent elevation in the content of NADPH oxidase and iNOS following cisplatin challenge or Cis NC administration was observed when compared with control. Also increases were more pronounced in the cisplatin intoxicated group compared with Cis NC administered rats. (Figure 4, $p < 0.05$).

The effect of Cis NC or cisplatin on inflammatory cytokines. In comparison with normal group, the levels of TNF- α and IL-1 β were significantly elevated in serum of cisplatin or Cis NC groups. However, the changes in the levels of inflammatory factors in the Cis NC treated group showed relatively reduced levels when compared to the cisplatin group (Figure 5, $p < 0.05$).

The effect of Cis NC or cisplatin on NF- κ B gene expression. To confirm the involvement of cisplatin or Cis NC in the changes induced in inflammatory mediators, we further estimated NF- κ B gene expression levels which increased significantly by cisplatin challenge or Cis NC administration

Table 2. The effect of Cis NC or cisplatin on the renal function test of normal male rats.

Groups parameters	Urea (mg/dL)	Creatinine (mg/dL)
Control	31.7 \pm 5.1	0.16 \pm 0.021
Cisplatin	64.8 \pm 3.8 ^a	0.70 \pm 0.159 ^a
Cis NC	33.8 \pm 4.1 ^b	0.25 \pm 0.022 ^b

Each value represents the mean \pm standard error of 10 records.

^asignificantly different from the control group at ($p \leq 0.05$).

^bsignificantly different from the cisplatin group at ($p \leq 0.05$).

above the levels observed in control. However, the level of NF- κ B gene expression in the Cis NC group is less manifested compared with the Cisplatin group (Figure 6, $p < 0.05$)

Effect of Cis NC or cisplatin on STAT1 gene expression in renal tissue. STAT1 is an essential constituent of inflammatory and apoptotic signal pathways and shows a key role in regulating numerous cellular stresses. Cisplatin intensely augmented the expression of STAT1 above its detected levels in Cis NC or normal renal tissue (Figure 7).

Effect of Cis NC or cisplatin on p53 gene expression in renal tissue. The p53 tumor suppressor protein shows a key role in regulating numerous cellular stresses and cell apoptosis. Cisplatin caused a greater increase in the expression of p53, than in Cis NC when compared to control (Figure 8).

The effect of Cis NC or cisplatin on caspase 3 level in renal tissue. In order to study the apoptotic influence of cisplatin or Cis NC, we measured the content of executioner caspase-3 by ELISA in renal tissue, where cisplatin induced greater activation of the caspase-3 level compared to control or Cis NC treated groups (Figure 9).

The effect of Cis NC or cisplatin on the AMPK/PI3K/Akt and mTOR signaling pathways in renal tissue. Figure 10(A) and (B) illustrated that the expression of p-AMPK, p-PI3K also p-Akt were reduced after cisplatin intoxication. Remarkably, Cis NC slightly affects the expression of p-AMPK, p-PI3K, and p-Akt when compared to the cisplatin intoxicated group. Furthermore, the phosphorylated form of mammalian target of rapamycin (mTOR) also increased in the renal tissue of cisplatin or Cis NC treated rats compared to control rats. However, the changes in Cis NC treated rats are less manifested as compared to Cisplatin intoxicated rats. (Figure 10(A) and (B)).

Effect of Cis NC or cisplatin on renal histopathological changes. Histopathological alterations of the rat kidney were considered to evaluate the efficiency of Cis NC in protecting the kidney from the deleterious effects of free

Table 3. The effect of Cis NC or cisplatin on oxidative stress biomarkers in normal male rats.

Groups Parameters	MDA (nmol/g tissue)	GSH (μ mol/g tissue)	8-OHdG (ng/g tissue)
Control	31.85 \pm 8.22	66.99 \pm 1.84	2.27 \pm 0.19
Cisplatin	79.81 \pm 3.75 ^a	23.20 \pm 1.40 ^a	6.05 \pm 1.18 ^a
Cis NC	55.22 \pm 6.79 ^{a,b}	45.54 \pm 2.05 ^{a,b}	3.53 \pm 0.22 ^{a,b}

Each value represents the mean \pm standard error of 10 records.

MDA: malondialdehyde; 8-OHdG: 8-hydroxydeoxyguanosine; GSH: Reduced glutathione.

^asignificantly different from the control group at ($p \leq 0.05$).

^bsignificantly different from the cisplatin group at ($p \leq 0.05$).

cisplatin. Examination with a light microscope of kidney tissues in a normal rat showed a typical glomerular structure and renal tubular interstitial without indication of inflammatory infiltration or cell necrosis (Figure 11 (a)). The rat intoxicated with cisplatin revealed massive inter-tubular hemorrhage replaced some tubules with degenerative changes in the tubules (Figure 11(b)). Moreover, the renal tubules in some cases are expanded, in others replaced by massive leukocytes, which may be progressive to necrosis. In other rat kidneys treated with cisplatin dilated renal tubules were seen besides leukocyte infiltration. In addition, the renal cortex presented glomerular atrophy, the remaining glomerular tuft was atrophied owing to minor fibrosis, Bowman's space was widened, and the basement membrane was thickened (Figure 11(c), (d), and (e)). In comparison, Cis NC treatment revealed a normal structure devoid of degenerative modifications or necrosis. In some specimens, congested intertubular blood vessels with albuminous casts in renal tubules were shown (Figure 11(f) and (g)).

Discussion

Several methods have been tried to minimize toxicity and enhance the efficacy of cisplatin, one of which is to apply nano-technology as a means of drug delivery method. Chitosan is one of the most plentiful natural polysaccharides, it has been considered comparatively safe because of its biodegradable and biocompatible properties, thus increasing its biomedical applications as drug delivery systems.^{30,31} In this study, we demonstrated that Cisplatin Nano Composite efficiently manifested lower side effects on renal tissue, it has less nephrotoxic impact compared with cisplatin. Cisplatin induced kidney damage by triggering inflammation, oxidative stress, and apoptosis and the fundamental molecular mechanisms can be via inhibition of AMPK/PI3K/Akt and stimulation of mTOR, STAT1/p53 signaling pathways.

Cisplatin nephrotoxicity is mediated by different cellular events, including DNA injury, reduced protein synthesis, mitochondrial dysfunction, and membrane peroxidation are due to failure to scavenge the produced

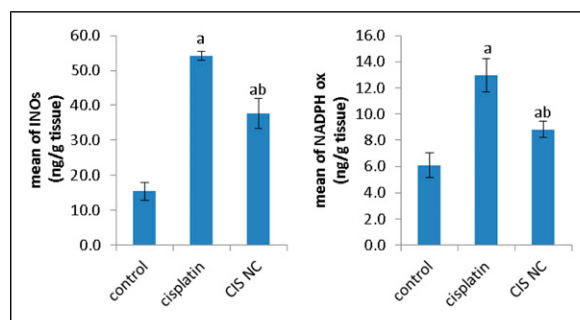


Figure 4. Effects of Cis NC or cisplatin on the levels of NADPH oxidase, and INOs. All values were expressed as mean \pm S.E. ^a $p < 0.05$ vs. normal group; ^b $p < 0.05$ vs. cisplatin group.

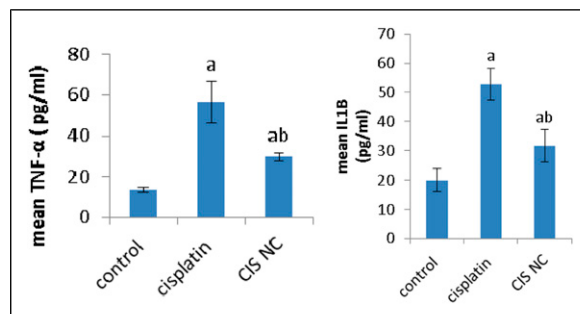


Figure 5. Effects of Cis NC or cisplatin on the content of inflammatory cytokines. All values were expressed as mean \pm S.E. ^a $p < 0.05$ vs. normal group; ^b $p < 0.05$ vs. cisplatin group.

free radical molecules in the body.³² In accordance with the preceding study,³³ our findings revealed that the morphological changes and kidney dysfunction represented by elevated levels of biomarkers of renal function tests including urea and creatinine caused by cisplatin challenge were associated with enhanced lipid peroxidation, GSH depletion, in addition to an increased accumulation of oxidative damage marker 8-OHdG, which may be a consequence of cisplatin-mediated increase in free radical generation or decreased redox potential of the mitochondria.³⁴ Thus the current induced oxidative stress cascade

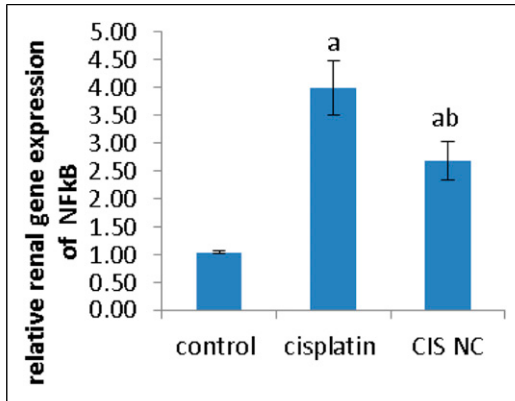


Figure 6. Effect of Cis NC or cisplatin on NF-κB gene expression level in renal tissue. All values were expressed as mean ± S.E. ^a $p < 0.05$ vs. normal group; ^b $p < 0.05$ vs. cisplatin group.

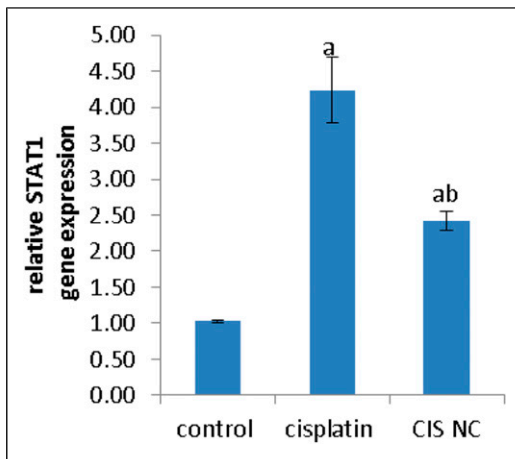


Figure 7. The effect of Cis NC or cisplatin on the gene expression levels of STAT1. All values were expressed as mean ± S.E. ^a $p < 0.05$ vs. normal group; ^b $p < 0.05$ vs. cisplatin group.

caused by cisplatin intoxication contributes to renal tubular damage in rats. Previous reports have also clarified that accumulative cisplatin causes the generation of great quantities of ROS in cells, which leads to the progress of oxidative stress, which is a dominant pathogenic element in cisplatin induced kidney injury.³⁵ However, we found a negligible increase in MDA levels, marginally decreased GSH levels, and a non-remarkable elevation in 8-OHdG in the Cis NC treated group as compared to the dramatic disturbance caused by cisplatin. It is obvious from our finding that Cis NC was not efficient in producing significant oxidative stress on normal renal cells, thus confirming its safety and biocompatibility. This finding was in agreement with Leekha et al.³⁶

As revealed during the present study, cisplatin increased renal NADPH oxidase in addition to iNOS protein expression. Current reports propose that, as well as ROS

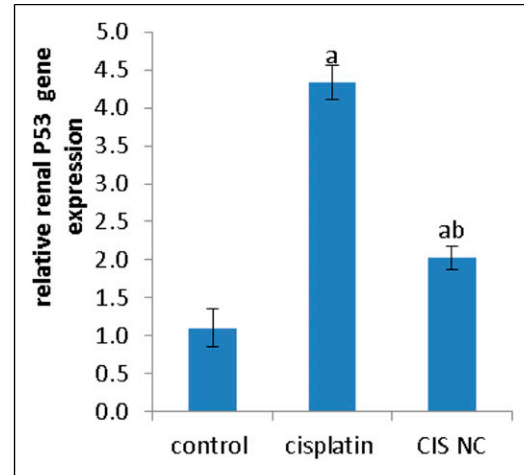


Figure 8. The effect of Cis NC or cisplatin on the gene expression levels of p53. All values were expressed as mean ± S.E. ^a $p < 0.05$ vs. normal group; ^b $p < 0.05$ vs. cisplatin group.

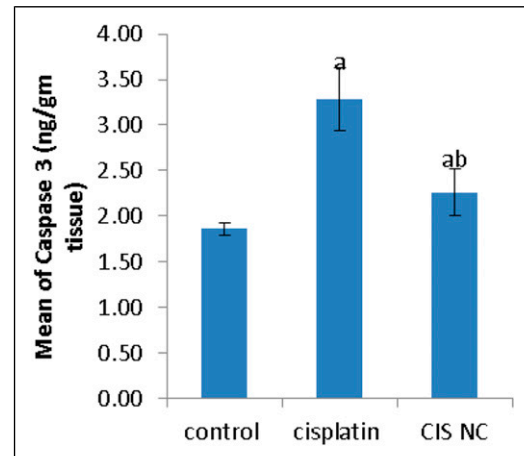


Figure 9. Effect of Cis NC or cisplatin on caspase 3 level in renal tissue. All values were expressed as mean ± S.E. ^a $p < 0.05$ vs. normal group; ^b $p < 0.05$ vs. cisplatin group.

mediated through NADPH oxidase expression, nitrosative stress plays a significant part in cisplatin induced nephrotoxicity.³⁷ Our results revealed that Cis NC treatment did not result in demonstrable changes in oxidative/nitrosative stress in renal tissue as compared with cisplatin.

In addition, there is evidence that locally produced ROS triggered the production of TNF- α post-renal injury, which through p38 MAPK activate NF-κB.⁷ Our data revealed activation of NF-κB associated with an elevated significant rise in the pro-inflammatory cytokines level including; IL-1 β and TNF- α in the serum of animals intoxicated with cisplatin as associated with the relative control. Also, the results obtained in this research involve upregulation of STAT1 in cisplatin mediated nephrotoxicity. Cisplatin

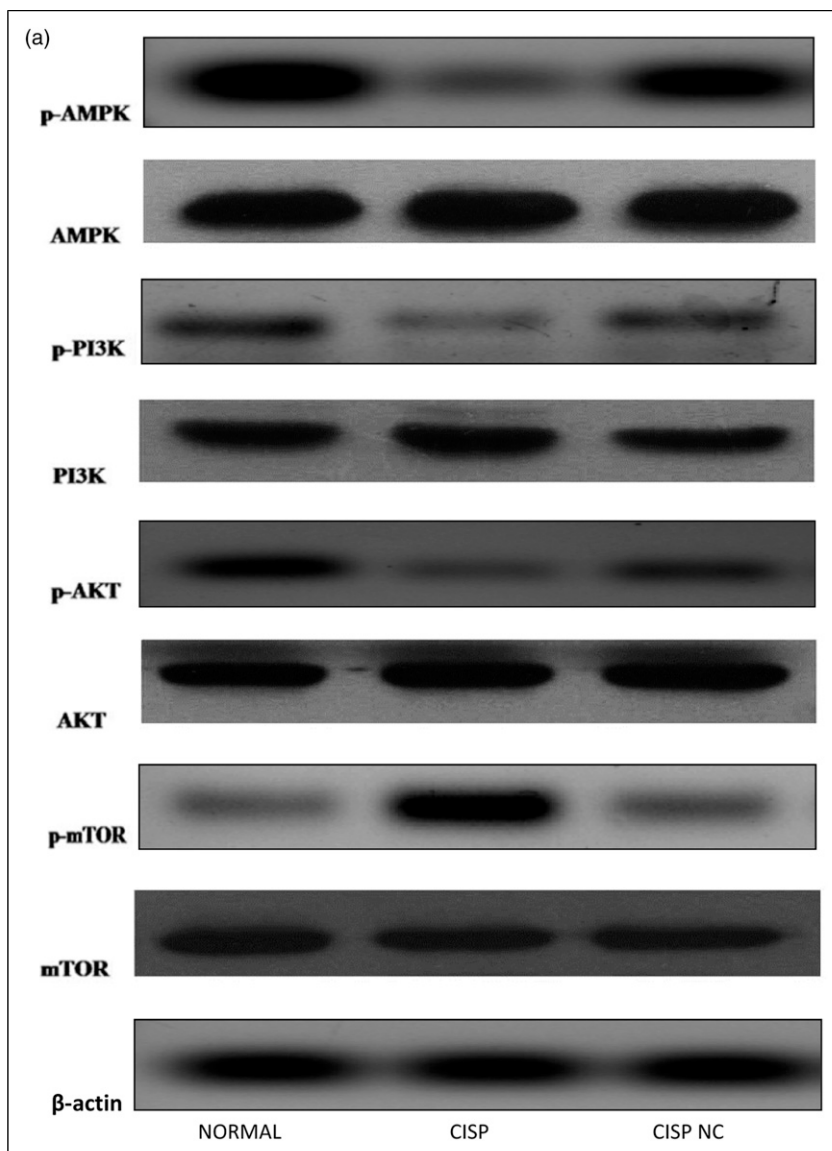


Figure 10. A, B. Effects of Cis NC or cisplatin on the protein expression level of AMPK/PI3K/Akt/mTOR signaling pathway along with the used loading control β -actin. Protein expression was estimated via quantitative analysis of relative protein expression in the kidney of each group of rats. The column charts show the ratio between the phosphorylated and total of the respective protein. Values were expressed as mean \pm S.E. $n=10$. ^a $p < 0.05$ vs. the normal group; ^b $p < 0.01$ vs. the cisplatin group.

activated STAT1 through ROS generation by means of NADPH oxidase. A variety of genes involved in inflammation were regulated by STAT1, such as iNOS,¹⁹ TNF- α ,²⁰ and p53.^{22,23} Consistent with our results these downstream effectors of STAT1, were elevated upon intoxication with cisplatin and contributed to the current cisplatin induced apoptosis and renal toxicity. We postulated that Cis NC exerted a minimal stimulatory effect on the inflammatory signal cascade and plays a promising part in modulating the effect of free cisplatin induced renal damage.

Apoptosis is a biological mechanism triggered by multiple variables and is also coordinated by a number of cell death signaling pathways.³⁸ Apoptotic machinery activation is linked to mitochondria, where p53 activation promotes the transcription of pro-apoptotic genes such as Bax, resulting in enhanced mitochondrial permeabilization and release of cytochrome c, which stimulates caspase-3 and initiates apoptosis via an oxidative stress related mitochondrial pathway.³⁹ It was confirmed that cisplatin-mediated renal injury was associated with cell apoptosis.⁹ we revealed that cisplatin

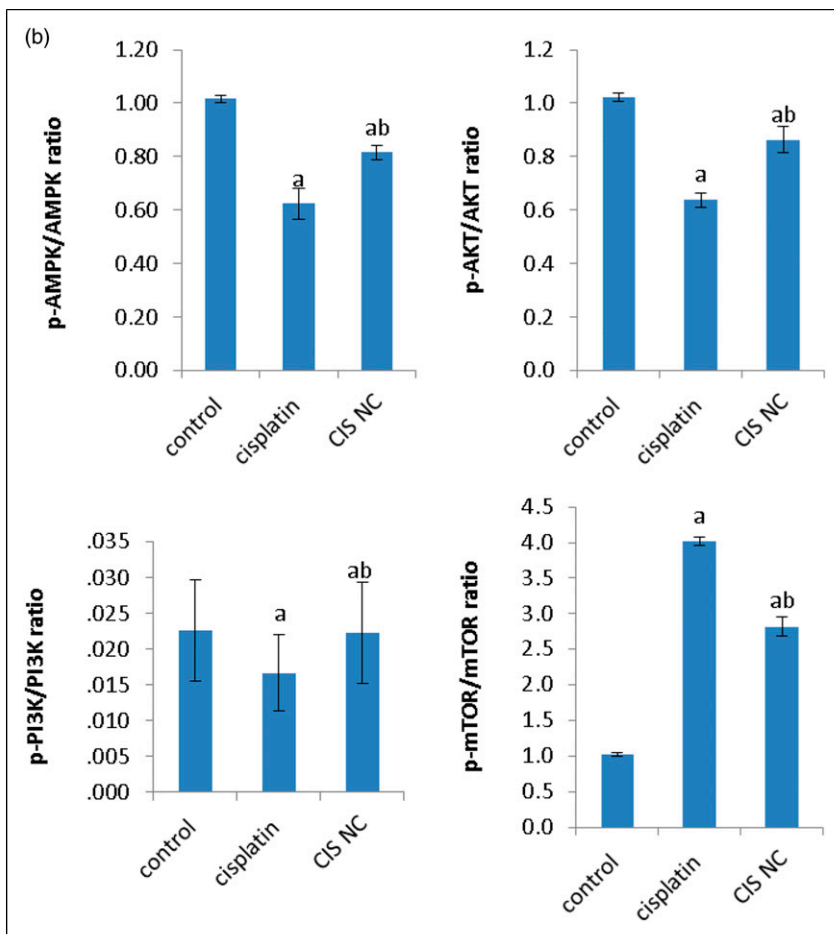


Figure 10. Continued.

induced activation of the executioner caspase-3 and p53, the upstream regulator of the apoptotic pathway, thus triggering cell apoptosis. Previous reports demonstrated that cisplatin challenge evoked apoptosis and inhibited the cell cycle in kidneys by suppressing the expression of Bcl-2 and increasing Bax and p53 expression; proposing that the inhibition of p53 activation may be a main objective for alleviating cisplatin nephrotoxicity.⁴⁰ Therefore, in this study, the gene expression of p53 was measured. The results indicated that the p53 protein expression level was significantly amplified after cisplatin intoxication, which was shown to a lesser extent in the group treated with Cis NC.

Earlier studies have also established that cisplatin induces apoptosis via AMPK-mediated signaling pathways, which is crucial in the enhancement of cisplatin mediated renal damage.⁴¹ Therefore, cisplatin induced renal injury can be mitigated through AMPK stimulation.^{13,14} In addition, the downstream target of AMPK is the PI3K/Akt signal and is closely associated with survival and cell

growth. The PI3K/Akt signaling pathway's role in renal damage is debatable; several researchers have established that stimulation of PI3K/Akt was associated with renal damage and was correlated with the generation of abundant ROS as well as apoptosis following cisplatin administration,^{10,42} whereas others found that the PI3K/AKT signaling pathway was inhibited following cisplatin administration and was associated with mitochondrial dysfunction.⁴³ Our current study postulated that cisplatin treatment caused inhibition of AMPK/PI3K/Akt expression in renal tissue, which was reliable with earlier results.¹³ Also, we confirmed that Cis NC treatment possesses a less inhibitory effect on the phosphorylation cascades of AMPK/PI3K/Akt when compared to cisplatin. As protein synthesis and cell growth are controlled by the essential regulator mTOR which is controlled via its upstream regulator PI3K/Akt.⁴⁰ We investigated the influence of cisplatin or Cis NC on mTOR stimulation; we found that Cis NC treatment showed no significant increased phosphorylation of mTOR compared to free cisplatin. PI3K/Akt

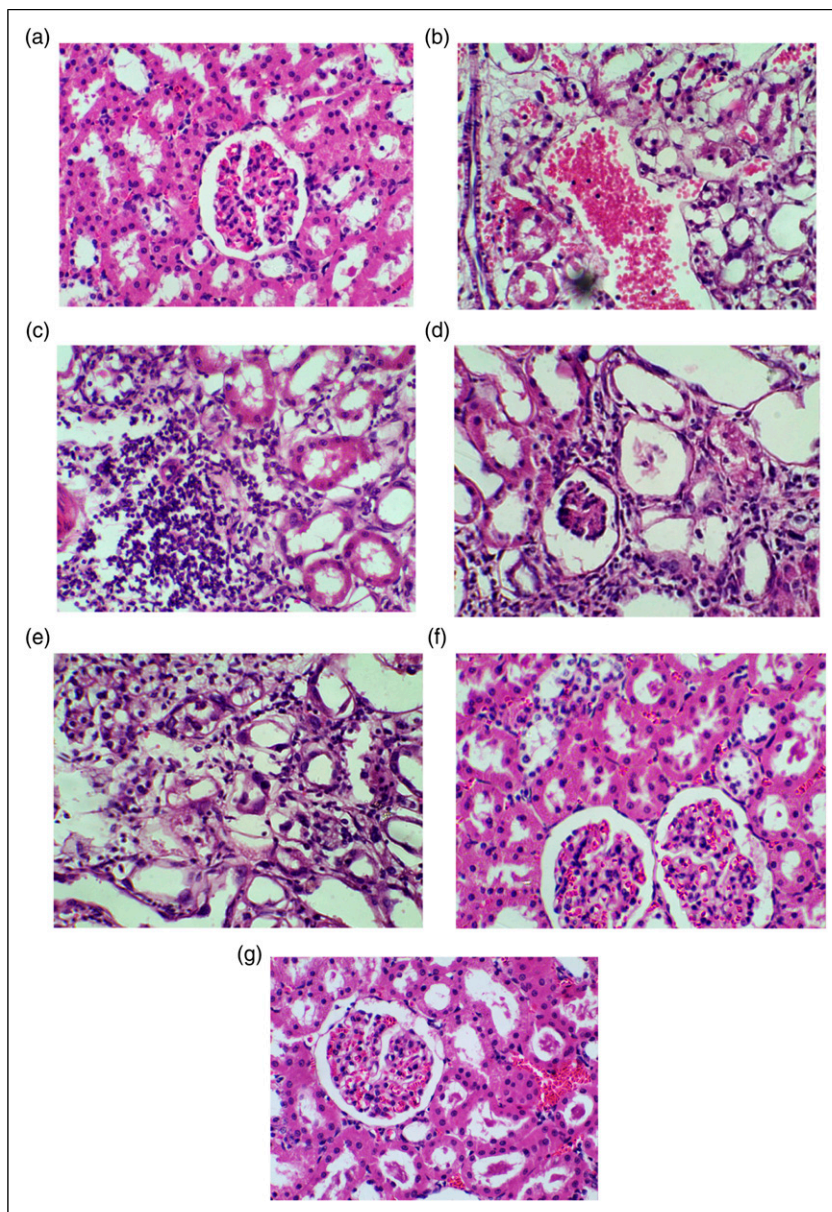


Figure 11. a; The kidney of a control rat shows normal structure (H& E \times 400), b; The kidney of a cisplatin rat presents massive intertubular hemorrhage replacing some tubules with degenerative changes in the tubules (H& E \times 400), c; The kidney of a cisplatin administered rat revealed extended renal tubules and other tubules replaced by massive leukocytes (H& E \times 400), d; The kidney of a cisplatin rat shows glomerular atrophy, widened capsular spaces, dilated renal tubules, and leukocyte infiltration (H& E \times 400), e; The kidney of a cisplatin administered rat shows degenerative changes of renal epithelium which progressive to necrosis of tubules and other loss of its details (H& E \times 400), f; kidney of the Cis NC rat with normal renal tissues (H& E \times 400), and g; The kidney of the Cis NC rat shows normal renal tissues with congested intertubular blood vessels with albuminous casts in the renal tubules (H& E \times 400).

can be positively activated by its direct regulator AMPK, the AMPK pathway can be suppressed by triggering ROS, causing inhibition of its downstream substrate PI3K/Akt phosphorylation, also AMPK is a negative regulator of mTOR, we demonstrated that cisplatin challenge caused inhibition of AMPK, resulting in mTOR over-activation. Researches on animal models demonstrated that the mTOR

signaling pathway was activated in chronic kidney disease, where mTOR increases pro-inflammatory and pro-fibrotic cytokines expression in addition to the infiltration of inflammatory cells in the interstitium, leading to renal function damage. Obviously, activation of AMPK and inhibition of mTOR ameliorate the progression of renal injury induced upon cisplatin challenge in different

models.^{14,44} Several studies have confirmed that PI3K/Akt regulates the Bcl-2 anti-apoptotic protein expression and is an upstream effector of p53.^{45,46} Therefore we postulated that induced kidney cell apoptosis by cisplatin may be via inhibition of AMPK activity and its downstream survival signal PI3K/Akt with triggered activation of p53 and the executioner caspase 3, this effect is less pronounced by Cis NC on renal cells.

Cisplatin intoxicated rats revealed condensation of kidney cell necrosis and protein cast, as well as vacuolization of the renal cortex, where Cis NC shows relatively normal architecture without degenerative changes or necrosis. All these collective results suggest that Cis NC exerted potential renal protection compared to free cisplatin. Previous studies have also examined the impact of cisplatin loaded nanocarriers on cells in comparison with cisplatin, and the findings demonstrated that cisplatin treated renal cells revealed a greater percentage of apoptotic and necrotic cells compared to the cisplatin loaded Nano-carriers,⁵ which is in agreement with the current study.

The results of this work indicated that preparation of cisplatin Nano-composite may decrease cisplatin kidney injury; this is probably owing to the gradual release of cisplatin from the Nano-carriers and decreased cisplatin toxicity on renal cells, thus reserving the renal structure and function.

However, more research is needed to identify the drug toxicity, and effectiveness of the formulated Nano-composite on further in-vivo and large scale of cell lines, in addition to the need of combined treatment with novel designed Nano-antioxidants⁴⁷ to reduce oxidative stress related toxicity of cisplatin. Also, understanding of biological processes and available studies concerning the pharmacokinetics and bioavailability of newly designed Nano based drugs should be considered to develop an appropriate treatment strategy. Furthermore, recent advances in nanotechnology have resulted in the development of a Nano-carrier based cisplatin in a various designated forms such as polymeric NPs, lipid-based Nano formulations, inorganic NPs, and carbon-based NPs, under preclinical and clinical phase trials with innovative impact in cancer treatment targeting with increased safety margin and minimized toxicity to normal cells.⁴⁸

Conclusions

We can conclude that Cis NC may be a valued promising agent to minimize nephrotoxicity induced by cisplatin where it exerts a minimal disrupting effect on redox balance in renal tissue, and less inhibitory effect on AMPK activity, and its downstream survival signal PI3K/Akt with a low stimulatory effect on expression of mTOR and

STAT1/P53 dependent apoptotic and inflammatory signaling pathways. However, future additional preclinical studies are needed to elucidate the beneficial effects of using Nano-based drugs to improve bioavailability and reduce drug toxicity.

Declarations

Acknowledgements

We wish to acknowledge the contribution of Dr Faten Ismail Abou El Fadl associate Prof. of chemistry, *National Center for Radiation Research and Technology (NCRRT), Egyptian Atomic Energy Authority, Cairo, Egypt*. For her assistance in preparation, examination, and interpretation of the nano characteristics of this work.

Declaration of conflicting interests

The author(s) declared no potential conflicts of interest with respect to the research, authorship, and/or publication of this article.

Funding

The author(s) received no financial support for the research, authorship, and/or publication of this article.

Consent for publication

Was provided to SAGE.

Availability of data and materials

All data generated or analyzed during this study is included in this article.

Ethics approval

All animal experiments were carried out in accordance with the National Institutes of Health guide for the Care and Use of Laboratory Animals (serial: 18–2019) in accordance with international ethical considerations.

Animal welfare

The present study followed international and national guidelines for animal treatment and complied with relevant legislation.

ORCID iD

Lobna.M Anees  <https://orcid.org/0000-0001-9730-1237>

References

1. Yao X, Panichpisal K, Kurtzman N, et al. (2007) Cisplatin nephrotoxicity: a review. *Am J Med Sci* 334: 115–124. DOI: [10.1097/MAJ.0b013e31812dfe1e](https://doi.org/10.1097/MAJ.0b013e31812dfe1e).
2. Pabla N and Dong Z (2008) Cisplatin nephrotoxicity: mechanisms and renoprotective strategies. *Kidney Int* 73: 994–1007. DOI: [10.1038/sj.ki.5002786](https://doi.org/10.1038/sj.ki.5002786).

3. Mehmood RK, Parker J, Ahmed S, et al. (2014) Review of cisplatin and oxaliplatin in current immunogenic and monoclonal antibodies perspective. *World Journal of Oncology* 5: 97–108.
4. Oberoi HS, Nukolova NV, Kabanov AV and Bronich TK (2013) Nanocarriers for delivery of platinum anticancer drugs. *Adv Drug Deliv Rev* 65: 1667–1685.
5. Trummer R, Rangsimawong W, Sajomsang W, et al. (2018) Chitosan-based self-assembled nanocarriers coordinated to cisplatin for cancer treatment. *RSC Adv* 8: 22967–22973.
6. Fard JK, Hamzei H, Sattari M, et al. (2016) Triazole rizatriptan induces liver toxicity through lysosomal/mitochondrial dysfunction. *Drug Research* 66(9): 470–478.
7. Miller RP, Tadagavadi RK, Ramesh G, et al. (2010) Mechanisms of Cisplatin nephrotoxicity. *Toxins* 2: 2490–2518. DOI: [10.3390/toxins2112490](https://doi.org/10.3390/toxins2112490).
8. Chirino YI and Pedraza-Chaverri J (2009) Role of oxidative and nitrosative stress in cisplatin-induced nephrotoxicity. *Exp Toxicol Pathol : Official Journal of the Gesellschaft Fur Toxikologische Pathologie* 61: 223–242.
9. Kong D, Zhuo L, Gao C, et al. (2013) Erythropoietin protects against cisplatin-induced nephrotoxicity by attenuating endoplasmic reticulum stress-induced apoptosis. *J Nephrol* 26: 219–227.
10. Potočnjak I and Domitrović R (2016) Carvacrol attenuates acute kidney injury induced by cisplatin through suppression of ERK and PI3K/Akt activation. *Food Chem Toxicol* 98: 251–261. DOI: [10.1016/j.fct.2016.11.004](https://doi.org/10.1016/j.fct.2016.11.004).
11. Duan B, Zhao Z, Liao W, et al. (2017) Antidiabetic effect of tibetan medicine Tang-Kang-Fu-San in db/db Mice via Activation of PI3K/Akt and AMPK Pathways. *Front Pharmacol* 8: 535.
12. Ke R, Xu Q, Li C, et al. (2018) Mechanisms of AMPK in the maintenance of ATP balance during energy metabolism. *Cell Biol Int* 42: 384–392. DOI: [10.1002/cbin.10915](https://doi.org/10.1002/cbin.10915).
13. Kim T-W, Kim Y-J, Kim H-T, et al. (2016) NQO1 deficiency leads enhanced autophagy in cisplatin-induced acute kidney injury through the AMPK/TSC2/mTOR Signaling Pathway. *Antioxidants Redox Signal* 24: 867–883.
14. Li J, Gui Y, Ren J, et al. (2016) Metformin protects against cisplatin-induced tubular cell apoptosis and acute kidney injury via AMPK α -regulated autophagy induction. *Sci Rep* 6(6): 23975. DOI: [10.1038/srep23975](https://doi.org/10.1038/srep23975).
15. Miao B and Degterev A (2011) Targeting phosphatidylinositol 3-kinase signaling with novel phosphatidylinositol 3,4,5-triphosphate antagonists. *Autophagy* 7(6): 650–651. DOI: [10.4161/auto.7.6.15248](https://doi.org/10.4161/auto.7.6.15248).
16. Reif S, Lang A, Lindquist JN, et al. (2003) The role of focal adhesion kinase-phosphatidylinositol 3-kinase-akt signaling in hepatic stellate cell proliferation and type I collagen expression. *J Biol Chem* 278: 8083–8090.
17. BahramiKhazaei AM, Khazaei M, Shahidsales S, et al. (2017) The therapeutic potential of PI3K/Akt/mTOR inhibitors in breast cancer: rational and progress. *J Cell Biochem* 119(1): 213–222. DOI: [10.1002/jcb.26136](https://doi.org/10.1002/jcb.26136).
18. Bian S, Sun X, Bai A, et al. (2013) P2X7 integrates PI3K/AKT and AMPK-PRAS40-mTOR signaling pathways to mediate tumor cell death. *PLoS One* 8: e60184.
19. Ohmori Y and Hamilton TA (2001) Requirement for STAT1 in LPS-induced gene expression in macrophages. *J Leukoc Biol* 69: 598–604.
20. Sugawara I, Yamada H and Mizuno S (2004) STAT1 knockout mice are highly susceptible to pulmonary mycobacterial infection. *Tohoku J Exp Med* 202: 41–50.
21. Yoshimura A (2006) Signal transduction of inflammatory cytokines and tumor development. *Cancer Sci* 97: 439–447.
22. Porta C, Hadj-Slimane R, Nejmeddine M, et al. (2005) Interferons α and γ induce p53-dependent and p53-independent apoptosis, respectively. *Oncogene* 24: 605–615.
23. Kaur T, Mukherjea D, Sheehan K, et al. (2011) Short interfering RNA against STAT1 attenuates cisplatin-induced ototoxicity in the rat by suppressing inflammation. *Cell Death Dis* 2: e180. DOI: [10.1038/cddis.2011.63](https://doi.org/10.1038/cddis.2011.63).
24. Yoshioka T, Kawada K, Shimada T, et al. (1979) Lipid peroxidation in maternal and cord blood and protective mechanism against activated-oxygen toxicity in the blood. *Am J Obstet Gynecol* 135: 372–376.
25. Beutler E, Duron O and Kelly BM (1963) Improved method for the determination of blood glutathione. *J Lab Clin Med* 61(5): 882–888.
26. Pfaffl MW (2001) A new mathematical model for relative quantification in real-time RT-PCR. *Nucleic Acids Res* 29(9): 45e–45. 1. DOI: [10.1093/nar/29.9.e45](https://doi.org/10.1093/nar/29.9.e45).
27. Charan J and Kantharia N (2013) How to calculate sample size in animal studies?. *J Pharmacol Pharmacother* 4(4): 303–306. DOI: [10.4103/0976-500X.119726](https://doi.org/10.4103/0976-500X.119726).
28. Selvam NCS, Kumar RT, Kennedy LJ, et al. (2011) Comparative study of microwave and conventional methods for the preparation and optical properties of novel MgO-micro and Nano-structures. *J Alloys Compd* 509(41): 9809–9815.
29. Abdel Ghaffar AM, Abou El Fadl FI and El-Sawy NM (2020) Radiation synthesis of polyvinyl alcohol/acrylic acid/magnesium oxide composite hydrogel for removal of boron from its aqueous solution. *J Thermoplast Compos Mater*: 1–19. DOI: [10.1177/0892705720925142](https://doi.org/10.1177/0892705720925142).
30. Gupta KC and Ravi Kumar MN (2001) pH dependent hydrolysis and drug release behavior of chitosan/poly(ethylene glycol) polymer network microspheres. *J Mater Sci Mater Med* 12(9): 753–759. DOI: [10.1023/a:1017976014534](https://doi.org/10.1023/a:1017976014534).
31. Cha J, Lee WB, Park CR, et al. (2006) Preparation and characterization of cisplatin-incorporated chitosan hydrogels, microparticles, and nanoparticles. *Macromol Res* 14(5): 573–578.
32. Dupre TV, Doll MA, Shah PP, et al. (2017) Inhibiting glucosylceramide synthase exacerbates cisplatin-induced acute kidney injury. *J Lipid Res* 58(7): 1439–1452.

33. Pedraza-Chaverri J, Sánchez-Lozada LG, Osorio-Alonso H, et al. (2016) New pathogenic concepts and therapeutic approaches to oxidative stress in chronic kidney disease. *Oxidative medicine and cellular longevity* 2016: 6043601.
34. Liu H-T, Wang T-E, Hsu Y-T, et al (2019) Nanoparticulated honokiol mitigates cisplatin-induced chronic kidney injury by maintaining mitochondria antioxidant capacity and reducing caspase 3-Associated Cellular apoptosis. *Antioxidants* 8(10): 466.
35. Marullo R, Werner E, Degtyareva N, et al. (2013) Cisplatin Induces a Mitochondrial-ROS Response That Contributes to Cytotoxicity Depending on Mitochondrial Redox Status and Bioenergetic Functions. *PLoS One* 8(11): e81162.
36. Leekha A, Kumar V, Moin I, et al. (2019) Modulation of Oxidative Stress by Doxorubicin Loaded Chitosan Nanoparticles. *Jcrp* 6(2): 76–84.
37. Sahu BD, Kalvala AKM, Mahesh Kumar J, et al. (2014) Ameliorative Effect of Fisetin on Cisplatin-Induced Nephrotoxicity in Rats via Modulation of NF- κ B Activation and Antioxidant Defence. *PLoS One* 9(9): e105070.
38. Muñoz-Pinedo C (2012) Signaling pathways that regulate life and cell death: evolution of apoptosis in the context of self-defense. *Adv Exp Med Biol* 738: 124–143.
39. Ahmadian E, Eftekhari A, Kavetsky T, et al. (2020) Effects of quercetin loaded nanostructured lipid carriers on the paraquat-induced toxicity in human lymphocytes. *Pestic Biochem Physiol* 167: 104586.
40. HuZhang SY, Zhang Y, Zhang M, et al. (2015) Aloperine Protects Mice against Ischemia-Reperfusion (IR)-Induced Renal Injury by Regulating PI3K/AKT/mTOR Signaling and AP-1 Activity. *Mol Med (N Y)* 21(1): 912–923.
41. Zhang L, Yang X, Li X, et al. (2015) Butein sensitizes HeLa cells to cisplatin through the AKT and ERK/p38 MAPK pathways by targeting FoxO3a. *Int J Mol Med* 36: 957–966.
42. Ju SM, Kang JG, Bae JS, et al. (2015) The Flavonoid Apigenin Ameliorates Cisplatin-Induced Nephrotoxicity through Reduction of p53 Activation and Promotion of PI3K/Akt Pathway in Human Renal Proximal Tubular Epithelial Cells. *Evid base Compl Alternative Med* 2015: 1–9. DOI: [10.1155/2015/186436](https://doi.org/10.1155/2015/186436).
43. Zhang J-J, Wang J-Q, Xu X-Y, et al. (2020) Red ginseng protects against cisplatin-induced intestinal toxicity by inhibiting apoptosis and autophagy via the PI3K/AKT and MAPK signaling pathways. *Food & Function* 11: 4236–4248.
44. Bao H, Zhang Q, Liu X, et al. (2019) Lithium targeting of AMPK protects against cisplatin-induced acute kidney injury by enhancing autophagy in renal proximal tubular epithelial cells. *Faseb J* 33(12): 14370–14381. DOI: [10.1096/fj.201901712R](https://doi.org/10.1096/fj.201901712R).
45. Zhang X, Wu H, Liu C, et al. (2015) PI3K/Akt/p53 pathway inhibits reovirus infection. *Infect Genet Evol* 34: 415–422.
46. Li X, Miao X, Wang H, et al. (2015) The tissue dependent interactions between p53 and Bcl-2 *in vivo*. *Oncotarget* 6: 35699–35709.
47. Eftekhari A, Dizaj SM, Chodari L, et al. (2018) The promising future of nano-antioxidant therapy against environmental pollutants induced-toxicities. *Biomed Pharmacother* 103: 1018–1027.
48. Farooq MA, Aquib M, Farooq A, et al. (2019) Recent progress in nanotechnology-based novel drug delivery systems in designing of cisplatin for cancer therapy: an overview. *Artificial Cells, Nanomedicine, and Biotechnology* 47(1): 1674–1692.